Coupled Plate Vibration Analysis using General Conditions of Boundary Restraint and Coupling Junction

Kavikant Mahapatra & S. K. Panigrahi

Deemed University

ABSTRACT

This paper presents the modelling and free vibration analysis of two elastically coupled plates in with general boundary conditions. Both out of plane and in-plane vibration are considered in in the present analysis thus making the methodology suitable for analysis of high frequency in-plane vibration along with low frequency bending characteristics. The plate displacement function has been derived using combination of trial beam functions , expressed as modified Fourier cosine series, in x and y direction. The modification of Fourier series is achieved by adding supplementary function to the basic Fourier series which has resulted in faster convergence rate of the series expansion. Finally, Rayleigh-Ritz method is employed to the Lagrangian function to derive the frequency matrix. The accuracy and effectiveness of the proposed method are validated through numerical examples and comparison with analytical and FEM results presented in literature.

Keywords: L-shape plates, elastic coupling, general boundary conditions, modified fourier cosine series, rayleigh-ritz method.

Classification: FOR Code: 091399

Language: English

London Journals Press

LJP Copyright ID: 392842
Print ISSN: 2631-8474
Online ISSN: 2631-8482

London Journal of Engineering Research

Volume 18 | Issue 2 | Compilation 1.0

Coupled Plate Vibration Analysis using General Conditions of Boundary Restraint and Coupling Junction

Kavikant Mahapatra[α] & S. K. Panigrahi[σ]

ABSTRACT

This paper presents the modelling and free vibration analysis of two elastically coupled plates in with general boundary conditions. Both out of plane and in-plane vibration are considered in in the present analysis thus making the methodology suitable for analysis of high frequency in-plane vibration along with low frequency bending characteristics. The plate displacement function has been derived using combination of trial beam functions , expressed as modified Fourier cosine series, in x and y direction. The modification of Fourier series is achieved by adding supplementary function to the basic Fourier series which has resulted in faster convergence rate of the series expansion. Finally, Rayleigh-Ritz method is employed to the Lagrangian function to derive the frequency matrix. The accuracy and effectiveness of the proposed method are validated through numerical examples and comparison with analytical and FEM results presented in literature.

Keywords: L-shape plates, elastic coupling, general boundary conditions, modified fourier cosine series, rayleigh-ritz method.

Author α σ: Department of Mechanical Engineering, DIAT (DU), Girinagar, Pune, Maharashtra, India-411025.

I. INTRODUCTION

Coupled two plate structure is an integral part of many engineering structure, mechanical system or dynamic mechanisms. These elements play a vital role in the design of marine, aerospace, mechanical and automobile structures. These structures also play a vital role in design of defence systems like armoured structures, ships hull structure, missile launchers etc. Hence, determination of the vibration characteristics of plate structures becomes crucial towards their anti-resonance design with respect to the external/internal excitation frequencies. In the existing literature of research, various analytical methods have been presented by researchers on vibration analysis of coupled plate system. Few of the earliest investigations have been carried out on structural power transmission and transmission of bending waves in coupled plate systems using the receptance method [1-3], Statistical Energy Analysis [4-5], mobility approach [6-7]. Bercin [8] used the Dynamic stiffness method and presented the effect of in-plane vibrations on energy flow in coupled plates. Travelling wave concept combined with modal solution approach was used by Kessissoglou [9] to analyse vibration characteristics of L shaped plates. Wang et al. [10] presented the substructure approach to study the vibration characteristics and power transmission in L-shaped plates. All the above studies were carried out on classical (ideal) boundary and coupling conditions. Modelling of real engineering structures do not exhibit ideal conditions at boundary and coupling junctions and exhibit some amount of relative linear and rotational motion at the boundary and coupled junctions. Hence modelling and analysis of structures with general boundary and coupling conditions is more of practical significance. One such method is to represent these non classical boundary conditions

incorporating elastic edge restraints using translational and rotational springs. Few of the existing literatures to have adopted these boundary conditions on coupled plate systems and undertaken analysis based on Fourier series expansion method are by Du et. al [11], Xu et.al [12], Chen et.al [13] and Shi et.al [14]. All the presented publications have used displacement assumption of Fourier series modified with an auxillary function. But there assumption of displacement function has resulted in a very large frequency matrix with many interrelated conditions for computation. This paper presents a simplified but computationally efficient modified Fourier series representation of displacement function to analyse the vibration characteristics of two coupled plate system. Four coupling formations have been considered i.e -90° (L shaped), -135°, -175° (very low angle coupling) and -180° (flat coupled plate). The presented methodology has resulted in significant reduction in the size of frequency matrix which in turn has led to faster computation of numerical results. Application of Rayleigh-Ritz proceedure to the Lagrangian function has been utilised to calculate the coefficients of the modified Fourier series. The effect of varying coupling conditions on natural frequency and mode shapes are investigated. Further, the correctness and accuracy of the method has been established by comparing the generated results with results presented in an earlier publication.

Such analysis is useful for prediction of dynamic response of plate structures with general boundary and coupling conditions. The methodology can be useful towards prediction of any variation of end supports and coupling junctions while in operation.

II. THEORETICAL FORMULATIONS

2.1 Description of the model

The Analytical models for the coupled two plates structure being investigated are composed of two elastic plates as shown in Fig.1. The boundary conditions at each uncoupled boundary has been represented as general condition using a linear spring ($\boldsymbol{K_{Tbend}}$) and torsional spring ($\boldsymbol{K_{Rbend}}$) for bending displacements and two linear springs ($\boldsymbol{K_{ni}}$ and $\boldsymbol{K_{ti}}$) in the x-y plane for in plane displacements. Similarly, at the coupling junction, four types of uniform coupling spring are introduced to completely model the coupling effect i.e one linear ($\boldsymbol{K_{CTb}}$) and torsion spring ($\boldsymbol{K_{CRb}}$) for bending restraint and two linear springs ($\boldsymbol{K_{Cni}}$ and $\boldsymbol{K_{Cti}}$) for longitudinal restraints. θ is the coupling angle of coupled plates structure. Thus, any variation in support conditions can be easily achieved in terms of change in rotational and/or linear spring stiffness's at the boundaries/ coupling junction. Further, the boundary conditions can be made ideal by taking infinite or zero values of spring stiffness's. Any finite value of stiffness would lead to a non-ideal boundary/ coupling condition.

The displacements of the elastic plates with respect to this coordinate system are described by u, v and w in the x, y and z directions, respectively. The coupling junction is taken as x_1=0 and x_2=0. The right hand coordinate system has been employed throughout the analysis.

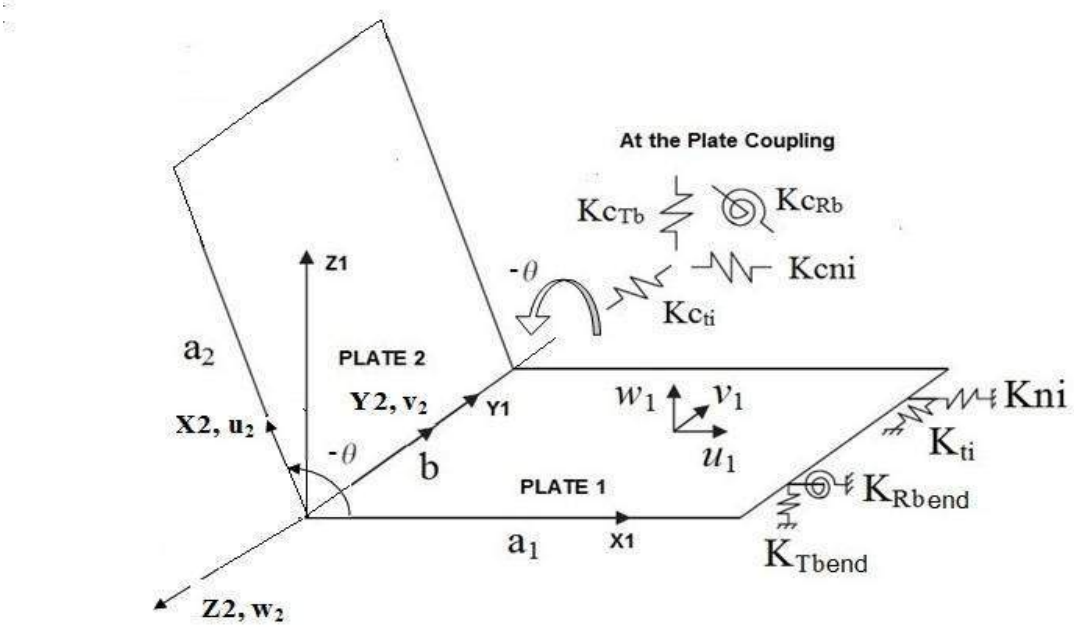

Figure 1: Coupled Two Plate System.

The coordinate system x_2,y_2,z_2 has been obtained by rotating $x_1,y_1\ z_1$ about Y_1 axis by –θ as dictated by right hand coordinate system. The relation between these two coordinate system can be derived as:

$$\begin{bmatrix} x_1 \\ y_1 \\ z_1 \end{bmatrix} = \begin{bmatrix} \cos(-\theta) & 0 & \sin(-\theta) \\ 0 & 1 & 0 \\ -\sin(-\theta) & 0 & \cos(-\theta) \end{bmatrix} \begin{bmatrix} x_2 \\ y_2 \\ z_2 \end{bmatrix} \quad (1)$$

III. THEORETICAL ANALYSIS FOR PLATE BENDING AND IN-PLANE VIBRATIONS

The theoretical formaulation for bending and in-plane vibration of plates has been presented for Plate 1. Plate 2 will follow the same derivation with coordinate system x_2,y_2,z_2, plate dimensions a_2, b_2 and respective material properties.

3.1 Energy Equation for Plate Bending and In-plane Vibrations

The Lagrangian equation for coupled plate system for free vibration can be expressed as

$$L = V - T \quad (2)$$

where L is the Lagrangian operator, V and T are the total potential and kinetic energy of the coupled plate system. According to the assumption of thin plate theory, the total potential and kinetic energy of the coupled plate system can be further expressed as

$$V = \sum_{k=1}^{2} V_{kbending} + \sum_{k=1}^{2} V_{k\,in-plane} + V_{12\,coupling}, \quad (3)$$

K is the plate number

$$T = \sum_{k=1}^{2} T_{kbending} + \sum_{k=1}^{2} T_{k\,in-plane} + V_{12\,coupling} + T_{2in-plane} \quad (4)$$

The expression for total potential energy includes energy associated with plate displacement as well as the total strain energies associated with the boundary springs. $V_{12\ coupling}$ represents the strain energy associated with the coupling springs at the plate junction.

For Plate 1 the expressions for V_1 , T_1 and $V_{12\ coupling}$ can be further expanded as

$$V_{1bending} = \frac{D_1}{2}\int_0^a\int_0^b \left\{\left(\nabla_1^{\,2} w_1\right)^2 + 2(1-\upsilon_1)\left[w_{1_{x_1y_1}}^{\,2} - w_{1_{x_1x_1}} w_{1\,y_1y_1}\right]\right\} dx_1 dy_1 + \frac{1}{2}\int_0^{b_1}\left[K_{Tbend x_1 0} w_1^{\,2} + K_{Rbend x_1 0} w_{1_{x_1}}^{\,2}\right]_{x_1=0} dy_1$$
$$+ \frac{1}{2}\int_0^{b_1}\left[K_{Tbend x_1 a_1} w_1^{\,2} + K_{Rbend x_1 a_1} w_{1_{x_1}}^{\,2}\right]_{x_1=a_1} dy_1 + \frac{1}{2}\int_0^{a_1}\left[K_{Tbend y_1 0} w_1^{\,2} + K_{Rbend y_1 0} w_{1_{y_1}}^{\,2}\right]_{y_1=0} dx_1 \quad (5)$$
$$+ \frac{1}{2}\int_0^{a_1}\left[K_{Tbend y_1 b_1} w_1^{\,2} + K_{Rbend y_1 b_1} w_{1_{y_1}}^{\,2}\right]_{y_1=b_1} dx_1$$

London Journal of Engineering Research

$$T_{1bending} = \frac{1}{2}\omega^2 \int_0^{a_1}\int_0^{b_1}\left[\rho_1 h_1 (w_1)^2\right] dx_1 dy_1 \tag{6}$$

$$V_{1in-plane} = \frac{G_1}{2}\int_0^{a_1}\int_0^{b_1}\left\{u_{1x_1}{}^2 + v_{1y_1}{}^2 + 2\upsilon_1 u_{1x_1} v_{1y_1} + \frac{1-\upsilon_1}{2}\left(u_{1y_1} + v_{1x_1}\right)^2\right\} dx_1 dy_1 + \frac{1}{2}\int_0^{b_1}\left[K_{nix_1 0} u_1{}^2 + K_{tix_1 0} v_1{}^2\right]_{x_1=0} dy_1$$
$$+ \frac{1}{2}\int_0^{b_1}\left[K_{nix_1 a_1} u_1{}^2 + K_{tix_1 a_1} v_1{}^2\right]_{x_1=a_1} dy_1 + \frac{1}{2}\int_0^{a_1}\left[K_{niy_1 0} v_1{}^2 + K_{tiy_1 0} u_1{}^2\right]_{y_1=0} dx_1 + \frac{1}{2}\int_0^{a_1}\left[K_{niy_1 b_1} v_1{}^2 + K_{tiy_1 b_1} u_1{}^2\right]_{y_1=b_1} dx_1 \tag{7}$$

$$T_{1in-plane} = \frac{1}{2}\rho_1 h_1 \omega^2 \int_0^{a_1}\int_0^{b_1}\left\{\left(u_1{}^2 + v_1{}^2\right)\right\} dx_1 dy_1 \tag{8}$$

$$V_{12coupling} = \frac{1}{2}\int_0^{b_1}\left\{\left[K_{CRb}\left(w_{1x_1}\big|_{x_1=0} - w_{2x_2}\big|_{x_2=0}\right)^2\right] + \left[K_{CTb}\left(w_{1x_1}\big|_{x_1=0} - w_{2x_2}\big|_{x_2=0}\cos(\theta) + u_{2x_2}\big|_{x_1=0}\sin(\theta)\right)^2\right]\right.$$
$$\left. + \left[K_{Cni}\left(u_{1x_1}\big|_{x_1=0} - u_{2x_2}\big|_{x_2=0}\cos(\theta) + w_{2x_2}\big|_{x_1=0}\sin(\theta)\right)^2\right] + \left[K_{Cti}\left(v_{1x_1}\big|_{x_1=0} - v_{2x_2}\big|_{x_2=0}\right)^2\right]\right\} dy_1 \tag{9}$$

where w_1 is the transverse displacement in the z_1-direction, u_1 and v_1 are the in-plane displacements in the x_1- and y_1- direction, respectively; ω is the angular frequency, $D_1 = \frac{E_1 h_1{}^3}{12(1-\upsilon_1{}^2)}$, $G_1 = \frac{E_1 h_1}{(1-\upsilon^2)}$, υ_1, ρ_1 and h_1 denote, respectively, the flexural rigidity, extensional rigidity, Poisson's ratio, mass density and the thickness of plates. E_1 denotes the Young's Modulus of plate 1.

$V_{12\ coupling}$ expression has been derived using displacement transformation of coordinates x_2 y_2 z_2 on coordinate system x_1 $y_1 z_1$.

$$\nabla_1 = \frac{\partial^2}{\partial x_1{}^2} + \frac{\partial^2}{\partial y_1{}^2}, \quad w_{1x_1x_1} = \frac{\partial^2 w_1}{\partial x_1{}^2}, \; w_{1y_1y_1} = \frac{\partial^2 w_1}{\partial y_1{}^2}, \; w_{1x_1y_1} = \frac{\partial^2 w_1}{\partial x_1 \partial y_1} \tag{10}$$

3.2 Fourier series expression for Displacement Function

The admissible functions for *w*, *u* and *v* play a very critical role in Rayleigh Ritz formulation. The admissible displacement function of a plate is often taken as a product of beam displacement function in x,y and z direction having the same boundary condition in x and y direction. Hence, the displacements w_1 u_1 and v_1 of Plate 1can be expressed as

$$w_1 = w_1(x_1) w_1(y_1) \tag{11}$$

$$u_1 = u_1(x_1) u_1(y_1) \tag{12}$$

$$v_1 = v_1(x_1) v_1(y_1) \tag{13}$$

where $w_1(x)$, $u_1(x)$ and $v_1(x)$ are the beam displacement functions of x_1 and $w_1(y)$, $u_1(y)$ and $v_1(y)$ are the beam displacement functions in y_1 direction.

The individual beam displacement functions have now been assumed as a Fourier cosine series which has been modified by addition of an auxiliary function such that the possible discontinuities associated with Fourier cosine series are totally eliminated.

The assumed Fourier cosine series representation of the beam displacements in terms of x_1 and y_1 are given as:

$$w_1(x_1)=\sum_{m=0}^{\infty}A_{w_1 m}\cos\alpha_m x+q_{w1x1}(x_1)\quad\left(where\ \alpha_m=\frac{m\pi}{a_1}\right)\ 0\le x_1\le a_1 \tag{14}$$

$$u_1(x_1)=\sum_{m=0}^{\infty}B_{u_1 m}\cos\alpha_m x+q_{u1x1}(x_1)\quad\left(where\ \alpha_m=\frac{m\pi}{a_1}\right)\ 0\le x_1\le a_1 \tag{15}$$

$$v_1(x_1)=\sum_{m=0}^{\infty}C_{v_1 m}\cos\alpha_m x+q_{v1x1}(x_1)\quad\left(where\ \alpha_m=\frac{m\pi}{a_1}\right)\ 0\le x_1\le a_1 \tag{16}$$

The auxillary functions q_{w1x1}, q_{u1x1} and q_{v1x1} have been derived in terms of known parameters of the plate using the condition for eliminating the discontinuities associated with Fourier cosine series in state of bending and in-plane vibration.

The condition of continuity of cosine series for bending and in-plane vibration is expressed as

$$\frac{\partial^3 q_{w1x1}}{\partial x_1^3}(0)=\frac{\partial^3 w_1(x_1)}{\partial x_1^3}(0)=d_0,\ \frac{\partial^3 q_{w1x1}}{\partial x_1^3}(a_1)=\frac{\partial^3 w_1(x_1)}{\partial x_1^3}(a_1)=d_1,\ \frac{\partial q_{w1x1}}{\partial x_1}(0)=\frac{\partial w_1(x_1)}{\partial x_1}(0)=d_2,$$
$$\frac{\partial q_{w1x1}}{\partial x_1}(a_1)=\frac{\partial w_1(x_1)}{\partial x_1}(a_1)=d_4 \tag{17}$$

$$\frac{\partial q_{u1x1}}{\partial x_1}(0)=\frac{\partial u_1(x_1)}{\partial x_1}(0)=\alpha_0,\frac{\partial q_{u1x1}}{\partial x_1}(a_1)=\frac{\partial u_1(x_1)}{\partial x_1}(a_1)=\alpha_1 \tag{18}$$

$$\frac{\partial q_{v1x1}}{\partial x_1}(0)=\frac{\partial v_1(x_1)}{\partial x_1}(0)=\beta_0,\frac{\partial q_{u1x1}}{\partial x_1}(a_1)=\frac{\partial v_1(x_1)}{\partial x_1}(a_1)=\beta_1 \tag{19}$$

Considering the requirement of least derivable function and the boundary conditions for beam in bending and in-plane state, the auxiliary functions chosen for the beam displacements are chosen as trigonometric functions given by

$$q_{1w1x1}=c_{w_1 1}\sin x_1+c_{w_1 2}\cos(2x_1)+c_{w_1 3}\sin(2x_1)+c_{w_1 4}\cos x_1 \tag{20}$$

$$q_{1u1x1}=c_{u_1 0}+c_{u_1 1}x_1+c_{u_1 2}x_1^{\,2} \tag{21}$$

$$q_{1v1x1}=c_{v_1 0}+c_{v_1 1}x_1+c_{v_1 2}x_1^{\,2} \tag{22}$$

The second part of the derivation of the auxillary function deals with application of boundary conditions for bending and in-plane vibration to the individual beam function. The associated boundary condition for bending for a beam is given as:

at $x_1=0$:

$$\frac{K_{Tbendx_1 0}}{D_1}w_1(x_1)=\frac{\partial^3 w_1(x_1)}{\partial x^3},\qquad \frac{K_{Rbendx_1 0}}{D_1}\frac{\partial w_1(x_1)}{\partial x_1}=-\frac{\partial^2 w_1(x_1)}{\partial x^2} \tag{23}$$

at $x_1=a_1$:

$$\frac{K_{Tbendx_1 a_1}}{D_1}w_1(x_1)=-\frac{\partial^3 w_1(x_1)}{\partial x^3},\qquad \frac{K_{Rbendx_1 a_1}}{D_1}\frac{\partial w_1(x_1)}{\partial x_1}=\frac{\partial^2 w_1(x_1)}{\partial x^2} \tag{24}$$

London Journal of Engineering Research

The same can be replicated for y_1 with respective boundary elastic spring stiffnesses.

The boundary conditions for in-plane vibration for a beam in terms of x_1 are given by the expressions:

$$\frac{K_{nix_10}}{G_1}u_1(x_1)=\left(\frac{\partial u_1(x_1)}{\partial x_1}\right),\quad \frac{K_{tix_10}}{G_1}v_1(x_1)=\left(\frac{1-\upsilon_1}{2}\right)\left(\frac{\partial v_1(x_1)}{\partial x_1}\right)\qquad \text{at}\quad x_1=0 \tag{25}$$

$$\frac{K_{nix_1a_1}}{G_1}u_1(x_1)=\left(-\frac{\partial u_1(x_1)}{\partial x_1}\right),\quad \frac{K_{tix_1a_1}}{G_1}v_1(x_1)=\left(\frac{1-\upsilon_1}{2}\right)\left(-\frac{\partial v_1(x_1)}{\partial x_1}\right)\text{at}\quad x_1=a_1 \tag{26}$$

$$\frac{K_{tiy_10}}{G_1}u_1(y_1)=\left(\frac{1-\upsilon_1}{2}\right)\left(\frac{\partial u_1(y_1)}{\partial y_1}\right),\quad \frac{K_{niy_10}}{G_1}v_1(y_1)=\left(\frac{\partial v_1(y_1)}{\partial y_1}\right)\qquad \text{at}\quad y_1=0 \tag{27}$$

$$\frac{K_{tiy_1b_1}}{G_1}u_1(y_1)=\left(\frac{1-\upsilon_1}{2}\right)\left(-\frac{\partial u_1(y_1)}{\partial y_1}\right),\quad \frac{K_{ntiy_1b_1}}{G_1}v_1(y_1)=\left(-\frac{\partial v_1(y_1)}{\partial y_1}\right)\text{at}\quad y_1=b_1 \tag{28}$$

Using Equations (17-26), the beam displacement function in x_1 direction for bending and in- plane vibration is derived as

$$w_1(x_1)=\sum_{m=0}^{\infty}A_{1w_1m}\left(\cos\alpha_m x+\xi_{w_1a_1x_1}*H_{w_1a_1}{}^{-1}*Q_{w_1a_1m}\right)=\sum_{m=0}^{\infty}A_{1w_1m}X_{w1m}(x_1) \tag{29}$$

$$u_1(x_1)=\sum_{m=0}^{\infty}B_{1u_1m}\left(\cos\alpha_m x+\xi_{u_1a_1x_1}*H_{u_1a_1}{}^{-1}*Q_{u_1a_1m}\right)=\sum_{m=0}^{\infty}B_{1u_1m}X_{u1m}(x_1) \tag{30}$$

$$v_1(x_1)=\sum_{m=0}^{\infty}C_{1v_1m}\left(\cos\alpha_m x+\xi_{v_1a_1x_1}*H_{v_1a_1}{}^{-1}*Q_{v_1a_1m}\right)=\sum_{m=0}^{\infty}C_{1v_1m}X_{v1m}(x_1) \tag{31}$$

The expressions for the terms of one of the derived expression (Eq.(30)) is placed at **Appendix 'A'**. For the beam displacement functions in y_1 direction, we need to replace all x_1 terms and stiffness's of the beam in Eq.(29)- Eq.(31) with terms associated in y_1 direction. This will generate expressions for $w_1(y_1)$, $u_1(y_1)$ and $v_1(y_1)$.

Hence using beam displacement functions in Eq.(11)-Eq(13), the plate displacement function for Plate 1 and Plate 2 can be expressed as:

$$w_k=\sum_{m=0}^{\infty}\left(\sum_{k=1}^{2}A_{wkmn}X_{wkm}(x_k)Y_{wkn}(y_k)\right) \tag{32}$$

$$u_1=\sum_{m=0}^{\infty}\left(\sum_{k=1}^{2}B_{ukmn}X_{ukm}(x_k)Y_{ukn}(y_k)\right) \tag{33}$$

$$v_1=\sum_{m=0}^{\infty}\left(\sum_{k=1}^{2}C_{vkmn}X_{vkm}(x_k)Y_{vkn}(y_k)\right) \tag{34}$$

3.3 Solution for Natural Frequency

Substituting Eq.(32-34) in Eq.(3) and Eq.(4) will give the energy expressions for Plate 1 and 2. There after substitution of the energy equations into Eq.(2) and minimising the Lagrangian with respect to all unknown Fourier coefficients of the displacement functions equal to zero, we will get a group of linear equations which can be expressed in matrix form as

$$\left(\mathbf{K}-\frac{\rho h\omega^2}{D}\mathbf{M}\right)\mathbf{E}=0 \tag{35}$$

For a two plate system with six unknown Fourier coefficients, the **K** and **M** matrix will have a size of 6x6 with each element of the matrix having a size defined by series truncation term m=M and n=N. The expression for the terms of the first row of Eq. (35) is given at **Appendix 'B'**. The general formation of Eq.(35) is given as:

$$\mathbf{K}=\begin{bmatrix} \mathbf{K}_{1-1} & \mathbf{K}_{1-2} & \mathbf{K}_{1-3} & \mathbf{K}_{1-4} & \mathbf{K}_{1-5} & \mathbf{K}_{1-6} \\ \mathbf{K}_{2-1} & \mathbf{K}_{2-2} & \mathbf{K}_{2-3} & \mathbf{K}_{2-4} & \mathbf{K}_{2-5} & \mathbf{K}_{2-6} \\ \mathbf{K}_{3-1} & \mathbf{K}_{3-2} & \mathbf{K}_{3-3} & \mathbf{K}_{3-4} & \mathbf{K}_{3-5} & \mathbf{K}_{3-6} \\ . & . & . & . & . & . \\ . & . & . & . & . & . \\ . & . & . & . & . & . \\ . & . & . & . & . & . \\ \mathbf{K}_{6-1} & .. & .. & .. & .. & \mathbf{K}_{6-6} \end{bmatrix} \quad (36)$$

$$\mathbf{M}=\begin{bmatrix} \mathbf{M}_{1-1} & .. & \mathbf{M}_{1-6} \\ . & . & . \\ . & . & . \\ \mathbf{M}_{6-1} & .. & \mathbf{M}_{6-6} \end{bmatrix} \quad (37)$$

$$\mathbf{E}=\begin{bmatrix}\mathbf{w}_1 & \mathbf{w}_2 & \mathbf{u}_1 & \mathbf{v}_1 & \mathbf{u}_2 & \mathbf{v}_2\end{bmatrix}^{-1} \quad (38)$$

$$\mathbf{w}_1=\begin{bmatrix}A_{w100} & A_{w101} & .. & .. & .. & A_{w1MN}\end{bmatrix}^{-1} \quad (39)$$

In the Frequency equation matrix represented by Eq. (35) the stiffness values have been modified as defined by the boundary conditions:

$$\frac{K_{Tbend}}{D_1}=\overline{K}_{Tbend},\ \frac{K_{Rbend}}{D_1}=\overline{K}_{Rbend},\ \frac{K_{ni}}{G_1}=\overline{K}_{ni},\ \frac{K_{ti}}{G_1}=\overline{K}_{ti} \quad (40)$$

IV. RESULTS AND DISCUSSIONS

The numerical analysis has been carried out for plate configurations coupled at -90°, -135°, -175° and -180° (flat coupled plate) as defined by the coordinate system. The material properties and plate thickness (h) of both the plates have been assumed to be same and have values given as:

Plate thickness (h_1=h_2)=0.008m
E=2.16x1011 N/m²
υ=0.28
ρ=7800 kg/m³

The plate dimensions taken are a1=1.4m, b1=1.2m, a2=1m and b2=1.2m with coupled edge having the same dimension. The properties and dimensions have been kept same as taken by Du et.al [11] for the purpose of validation of results. The boundary conditions for the two plates have been set to near ideal simply supported for bending and clamped for inplane vibration modes and the analysis has been carried out to present the effect of variation of coupling stiffness and coupling angles on the vibration characteristics of the coupled system. The boundary conditions and plate angle configurations are presented in Fig. 2.

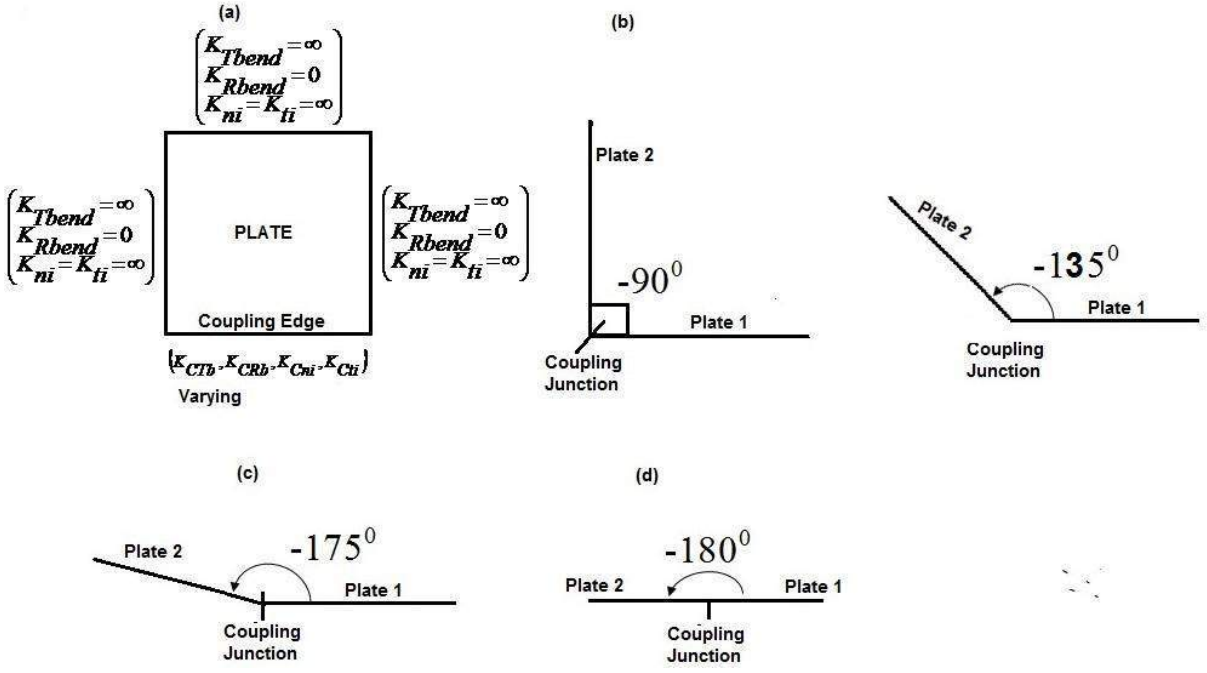

Figure 2: Boundary Condition and Coupling Angles (a) Boundary Condition (b) Coupling Angle=-90° (c) Coupling Angle=-175° (d) Coupling Angle=-180°

4.1 Validation and Convergence of Natural Frequency and corresponding Modes

The numerical results have been generated for the L shaped coupled plate configuration and validated with similar results obtained by Du et.al [11]. The boundary conditions and coupling edge have been taken as mentioned above. The coupling spring stiffness's used for analysis are K_{CRb} =1e4, K_{TRb} =1e4, K_{Cni} =1e5, K_{Cni} =1e4. The convergence and validation results for first four natural frequency for an L shaped coupled plate have been presented for different truncation schemes m=0,1,2...M and n=1,2,3..N in Table 1.

Table 1: Covergence and Validation of Natural Frequency

Mode No	Natural Frequency (Hz)					
	Present Method		Du et.al [11]			
	M=N=1	M=N=2	M=N=4	M=N=8	M=N=9	FEM
1	16.151	16.147	16.243	16.154	16.147	16.109
2	20.233	20.219	20.573	20.444	20.438	20.389
3	33.980	33.837	34.065	33.713	33.710	33.553
4	48.765	48.390	52.6	52.139	52.136	51.934

From Table 1, it can be seen that the results compare very well and accurate with the analytical and FEM results obtained by Du.et.al [11]. Also, the present method is far more efficient in convergence hence speed of calculation in comparison to the method used by Du. Et.al [11]. This efficiency is due to generation of a very small Frequency Matrix size (6x6) in the presented method as compared to the one generated in literature (38x38) being referred. For all our further analysis, truncation of Fourier expansion series at M,N=2 has been utilised. The corresponding modes for a coupled L shaped plate structure is presented in Fig. 3.

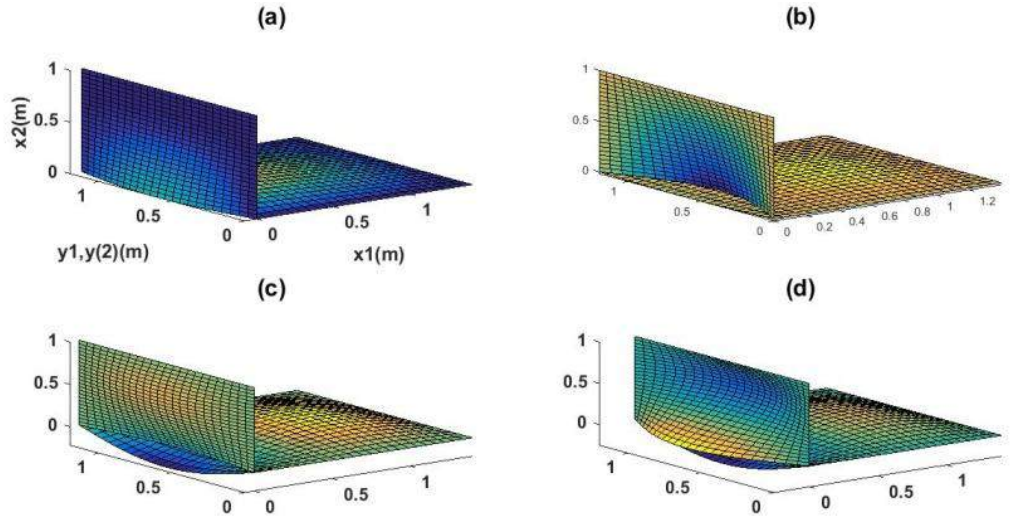

Figure 3: Mode Shapes for L shaped Coupled Plate with Coupling Spring Stiffness's K_{CRb} = 1e4, K_{TRb} = 1e4, K_{Cni} = 1e5, K_{Cni} = 1e4 (a) Mode 1 (b) Mode 2 (c) Mode 3 (d) Mode 4

From Fig. 3, it can be seen that because of consideration of elastic coupling, the coupling at the junction in the modes are no longer continuous and have a gap in comparison to rigid coupling mode. This is mainly because of soft coupling at the junction which is far less than the rigidity of the structure. This coupling condition results in a weak coupling between in- plane and out-of plane vibration thus resulting junction gap.

4.2 Variation of Natural Frequency with Coupling Rotational Spring Stiffness (K_{CRB})

Further, analysis has been undertaken to present the variation in natural frequency of an L shaped coupled plate system having simply supported boundaries and fully clamped junction (all junction stiffness's set to 10^{10}) while reducing the rotational spring stiffness at junction (K_{CRb}) gradually in steps to 0.

Table 2: Variation of Natural Frequency of an L Shaped Coupled Plate with Simply supported Boundaries and Clamped Coupling Configuration

^{K}CRb	Natural Frequency (Hz)			
	Mode 1	Mode 2	Mode 3	Mode 4
$_{10}10$	994.93	1101.86	1352.45	1651.72
10^7	175.81	186.44	1478.06	1558.65
10^6	61.051	87.205	1489.5	1551.27
10^4	24.7309	34.034	66.033	75.752
10^2	24.387	34.742	65.897	76.079
10	24.384	34.749	65.896	76.082
0	24.383	34.745	65.895	76.083

It can be seen from Table 2 that for extremely high values of coupling spring stiffness (>10^4), the L shaped coupled plate system behaves as a rigid body configuration exhibiting very high values of natural frequency. Between K=10^4 to 0, there is a very marginal decrease in the first natural frequency and marginal increase in 2nd, 3rd and 4th natural frequency. Thus K_{CRb}=10^4 sets the upper limit for a rigid coupling configuration. The corresponding modes for the first four natural frequencies for K = 10^4 is shown in Fig. 4.

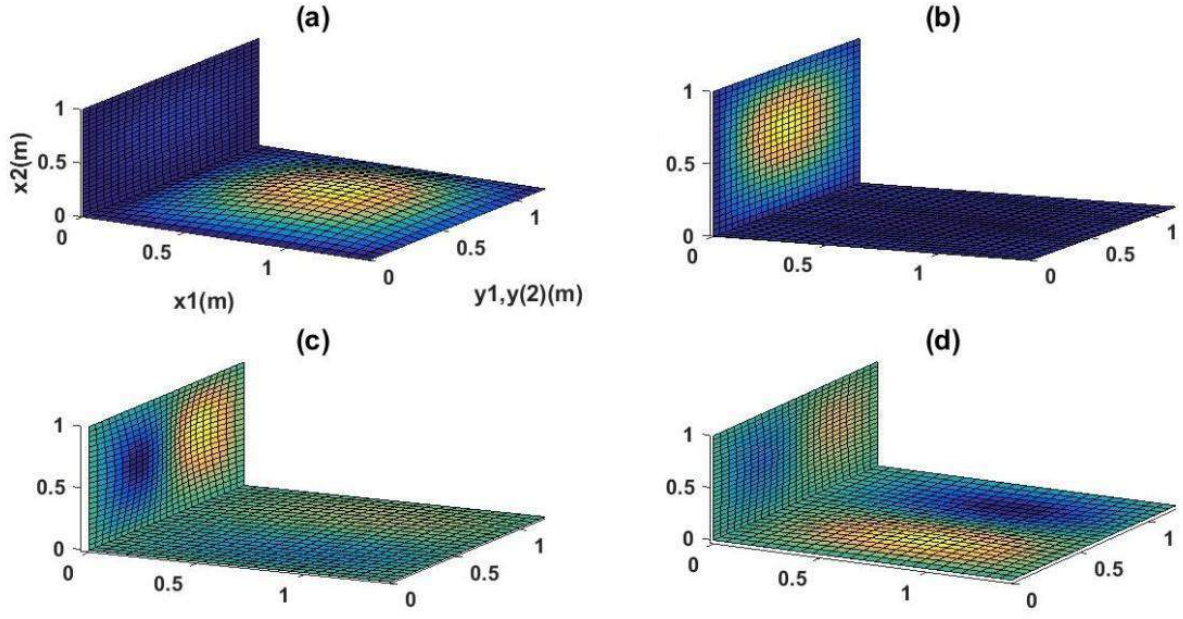

Figure 4: Mode Shapes for L shaped Coupled Plate with Rigid Coupling stifness's K_{CRb} = 1e4, K_{TRb} = 1e10, K_{Cni} = 1e10, K_{Cni} = 1e10 (a) Mode 1 (b) Mode 2 (c) Mode 3 (d) Mode 4

It can be observed from the Mode shapes in Fig. 4 that for rigid coupling configuration, the discontinuities at the coupling junction are no longer existing. Also, the vibration characteristics tend to appear on the entire plate structure.

4.2 Variation of Natural Frequency with Coupling Angle

To analyse the variation of natural frequency and mode shapes with varying angles of coupling, a soft spring coupling junction has been utilised with the spring stiffness's defined as K_{CRb} =1e4, K_{TRb} =1e4, K_{Cni} =1e5, K_{Cni} =1e4. Numerical results have been obtained for coupling angles -180°, -175°, -135° and -90°. The natural frequency obtained are presented in Table 3 and the corresponding comparison of the first mode in all 04 cases is presented in Fig. 5.

Table 3: Variation of Natural Frequency with Coupling Angle with Soft Coupling Junction

Coupling Angle	Mode 1	Natural Frequency (Hz)		Mode 4
		Mode 2	Mode 3	
-180°	16.15	17.625	33.999	47.273
-175°	16.15	17.648	33.999	47.284
-135°	16.11	19.022	33.948	48.048
-90°	16.148	20.219	33.837	48.390

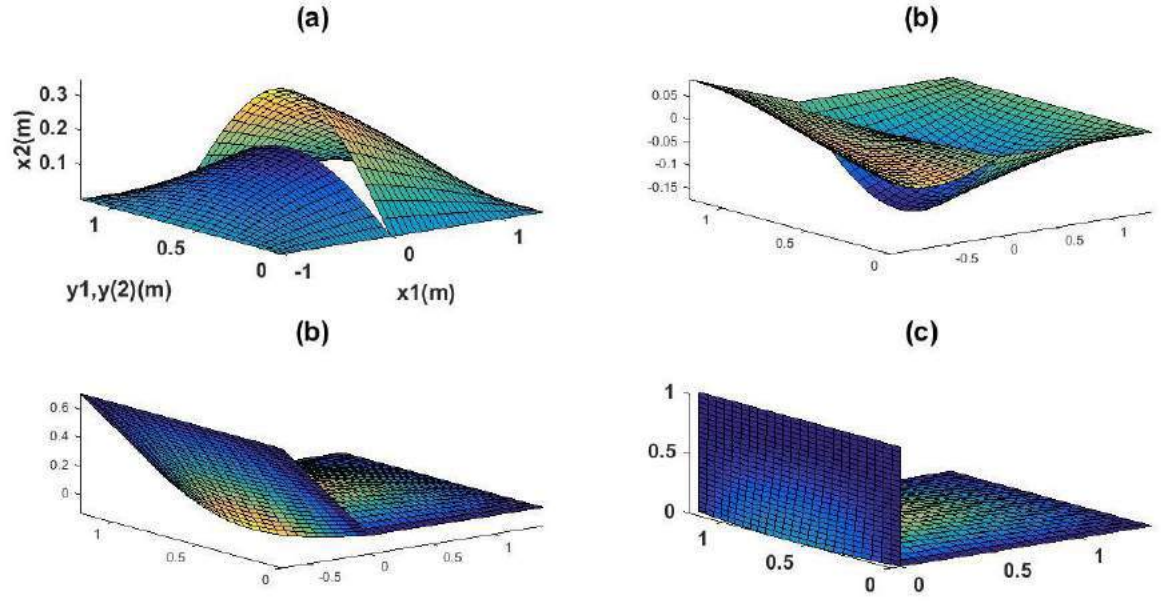

Figure 5: Comparison of First Mode with varying Coupling Angles for a coupled two Plate system having spring stiffness's representing a soft coupling junction (a) Coupling Angle=-180° (b) Coupling Angle=-175° (c) Coupling Angle=-135° (d) Coupling Angle=-90°

It can be inferred from Table 2 and Fig. 5 that although there is a marginal variation of natural frequency with variation of coupling angle, but the corresponding mode shape exhibits appreciable variation. This happens due to the interaction of bending and in-plane waves of the two plates interacting at different angles at the coupling junction . Further, in a flat coupled plate configuration the weak coupling junctions allows the two plates to move independently of each other.

V. CONCLUSION

(a) The inclusion of a new and simple auxiliary function in the assumed displacement equation for in-plane vibration of square plate has resulted in an highly accurate and rapid convergence of solution (frequency parameter) using the Rayleigh-Ritz approach. The numbers of terms in the frequency matrix have greatly reduced thus greatly decreasing the computational time and accuracy.

(b) The examples presented for combination of general coupling conditions of the coupled plate system have clearly brought out the impact of variation of junction stiffness and coupling angle on the vibrational characteristics (variation in frequency parameter) of the coupled plate system. The distinctive nature of modes with even slight variation of natural frequencies have led to the conclusion that coupled plate modes can be an effective tool to monitor and variation of the coupling junction properties. It is envisaged that the proposed methodology and the results can be useful as a reference for future research works involving more complex coupled structures with higher number of plates.

Appendix 'A'

$$\xi_{u_1 a_1 x_1} = \left[\frac{-x_1^{\,2}}{2a_1} + x_1 - \frac{a_1}{3} \qquad \frac{x_1^{\,2}}{2a_1} - \frac{a_1}{6} \right]$$

$$H_{u_1 a_1} = \begin{bmatrix} -\overline{K}_{nix_1 0}\left(\frac{a_1}{3}\right) - 1 & -\overline{K}_{nix_1 0}\left(\frac{a_1}{6}\right) \\ \overline{K}_{nix_1 a_1}\left(\frac{a_1}{6}\right) & \overline{K}_{nix_1 a_1}\left(\frac{a_1}{3}\right) + 1 \end{bmatrix}$$

$$Q_{u_1 a_1 m} = \begin{bmatrix} -\overline{K}_{nix_1 0} \\ -(-1)^m \overline{K}_{nix_1 a_1} \end{bmatrix}$$

Appendix 'B'

$$\mathbf{K}_{1-1} = \left(\int_0^{a_1} \int_0^{b_1} \left(\begin{matrix} X_{w1m}{}'' X_{w1i}{}'' Y_{w1n} Y_{w1j} + X_{w1m}{}' X_{w1i} Y_{w1n}{}'' Y_{w1j}{}'' + \upsilon X_{w1m}{}'' X_{w1i} Y_{w1n} Y_{w1j}{}'' + \upsilon X_{w1m} X_{w1i}{}'' Y_{w1n}{}'' Y_{w1j} \\ + 2(1-\upsilon) X_{w1m}{}' X_{w1i}{}' Y_{w1n}{}' Y_{w1j}{}' \end{matrix} \right) dx_1 dy_1 \right)$$

$$+ \int_0^{b_1} \overline{K}_{Tbend x_1 a_1} \left(X_{w1m} X_{w1i} Y_{w1n} Y_{w1j} \right)\Big|_{x=a_1} dy_1 + \int_0^{b_1} \overline{K}_{Rbend x_1 a_1} \left(X_{w1m}{}' X_{w1i}{}' Y_{w1n} Y_{w1j} \right)\Big|_{x=a_1} dy_1$$

$$+ \int_0^{a_1} \left\{ \overline{K}_{Tbend y_1 0} \left(X_{w1m} X_{w1i} Y_{w1n} Y_{w1j} \right)\Big|_{y_1=0} + \overline{K}_{Rbend y_1 0} \left(X_{w1m} X_{w1i} Y_{w1n}{}' Y_{w1j}{}' \right)\Big|_{y_1=0} \right\} dx_1$$

$$+ \int_0^{a_1} \left\{ \overline{K}_{Tbend y_1 b_1} \left(X_{w1m} X_{w1i} Y_{w1n} Y_{w1j} \right)\Big|_{y_1=b_1} + \overline{K}_{Rbend y_1 b_1} \left(X_{w1m} X_{w1i} Y_{w1n}{}' Y_{w1j}{}' \right)\Big|_{y_1=b} \right\} dx_1$$

$$+ \int_0^{b_1} \left(\frac{K_{CTb}}{D_1} \right) \left(X_{w1m} X_{w1i} Y_{w1n} Y_{w1j} \right)\Big|_{x_1=0} dy_1 + \int_0^{b_1} \frac{K_{CRb}}{D_1} \left(X_{w1m}{}' X_{w1i}{}' Y_{w1n} Y_{w1j} \right)\Big|_{x_1=0} dy_1$$

$$\mathbf{K}_{1-2}=\int_0^{b_1}-\frac{K_{CTb}}{D_1}\left(X_{w2m}\big|_{x_2=0}X_{w1i}\big|_{x_1=0}Y_{w1n}Y_{w1j}\right)\cos(\theta)dy_1+\int_0^{b_1}-\frac{K_{CRb}}{D_1}\left(X_{w2m}'\Big|_{x_2=0}X_{w1i}'\Big|_{x_1=0}Y_{w1n}Y_{w1j}\right)\cos(\theta)dy_1$$

$$\mathbf{K}_{1-3}=\mathbf{K}_{1-4}=\mathbf{K}_{1-6}=0$$

$$\mathbf{K}_{1-5}=\int_0^{b_1}\frac{K_{CTb}}{D_1}\left(X_{u2m}\big|_{x_2=0}X_{w1i}\big|_{x_1=0}Y_{w1n}Y_{w1j}\right)\sin(\theta)dy_1$$

$$\mathbf{M}_{1-1=}\frac{\rho_1 h_1\omega^2}{D_1}\int_0^{a_1}\int_0^{b_1}\left(X_{w1m}X_{w1i}Y_{w1n}Y_{w1j}\right)dx_1dy_1$$

$$\mathbf{M}_{1-2}=0,\ \mathbf{M}_{1-3}=0,\ \mathbf{M}_{1-4}=0,\ \mathbf{M}_{1-5}=0,\ \mathbf{M}_{1-6}=0$$

REFERENCES

1. Azimi, S., Hamilton, J. F. and Soedel, W. The receptance method applied to the free vibration of continuous rectangular plates. *Journal of Sound and Vibration,* 1984, **93,** 9-29.
2. Farag, N. H. and Pan, J. On the free and forced vibration of single and coupled rectangular plates. *Journal of the Acoustical Society of America,* 1998, **104,** 204-216.
3. Kim, H. S., Kang, H. J. and Kim, J. S. Transmission of bending waves in inter-connected rectangular plates. *Journal of the Acoustical Society of America,* 1994, **96,** 1557-1562.
4. Mace, B. R. and Rosenberg, J. The SEA of two coupled plates: an investigation into the effects of system irregularity. *Journal of Sound and Vibration*. 1999, **212,** 395- 415.
5. Dimitriadis, E. K. and Pierce, A. D. Analytical solution for the power exchange between strongly coupled plates under random excitation: a test of statistical energy analysis concepts. *Journal of Sound and Vibration*. 1988, **123,** 397-412.
6. Cuschieri, J. M. Structural power-flow analysis using a mobility approach of an L- shaped plate. *Journal of the Acoustical Society of America*. 1990,**87,** 1159-1165.
7. Cuschieri, J. M. and McCollum, M. D. In-plane and out-of-plane waves power transmission through L-plate junction using the mobility power flow approach *Journal of the Acoustical Society of America*. 1996, **100,** 857–870.
8. Bercin, A. N. An assessment of the effects of in-plane vibrations on the energy flow between coupled plates. *Journal of Sound and Vibration*. 1996, **191,** 661-680.
9. Kessissoglou, N. J. Power transmission in L-shaped plates including flexural and in-plane vibration. *Journal of the Acoustical Society of America*. 2004, **115,** 1157-1169.
10. Wang, Z. H., Xing, J. T. and Price, W. G. An investigation of power flow characteristics of L- shaped plates adopting a substructure approach. *Journal of Sound and Vibration*. 2002, **250,** 627-648.
11. Du J., Li W.L. and Liu Z. et al. Free vibration of two elastically coupled rectangular plates with uniform elastic boundary restraints. *Journal of Sound and Vibration*. 2011, **330,** 788–804.
12. Xu H., Li W.L. and Du J. Modal analysis of general plate structures. *J Vib Acoust*. 2013, **136,** 021002–021011.
13. Yuehua Chen, Guoyong Jin, Jingtao Du and Zhigang Liu. Vibration characteristics and power transmission of coupled rectangular plates with elastic coupling edge and boundary restraints. *Chinese journal of mechanical engineering*. 2012, **25(2),** 262- 276.
14. Shi Xianjie and Shi Dongyan. Free and forced vibration analysis of T-shaped plates with general elastic boundary supports. *Journal of Low Frequency Noise, Vibration and Active Control*. 2018, **37(2)**, 355–372.